Development and assessment of a water pressure reduction system for lining invert of underwater tunnels

Pengfei Li, Chunhui Feng, Hongchuan Liu, Yong Zhaoc, Zhen Li, Haocheng Xiong

Manuscrit accepté pour publication de : LI, Pengfei, FENG, Chunhui, LIU, Hongchuan, ZHAOC, Yong, LI, Zhen, XIONG, Haocheng, 2021, Development and assessment of a water pressure reduction system for lining invert of underwater tunnels, Marine Georesources & Geotechnology, 39, 3, Taylor & Francis Ltd, pp. 365-371
https://doi.org/10.1080/1064119X.2019.1703126

Development and Assessment of a Water Pressure Reduction System for Lining Invert of Tunnels in Saturated Grounds

Pengfei Li[a], Chunhui Feng[b], Hongchuan Liu[c], Yong Zhao[d], Zhen Li[e], Haocheng Xiong[f]*

a. Key Laboratory of Urban Security and Disaster Engineering, Ministry of Education, Beijing University of Technology, Beijing 100124, China; lpf@bjut.edu.cn

b. Key Laboratory of Urban Security and Disaster Engineering, Ministry of Education, Beijing University of Technology, Beijing 100124, China; 602542923@qq.com

c. Key Laboratory of Urban Security and Disaster Engineering, Ministry of Education, Beijing University of Technology, Beijing 100124, China; lpf@bjut.edu.cn; liuhonch@qq.com

d. Chinses Economic and Planning Research Institute of Railways, Beijing 100844, China; 452754371@qq.com

e. IFSTTAR, GERS, GMG, Allée des Ponts et Chaussées, Bouguenais, France; zheng.li@ifsttar.fr

f. Corresponding Author National Center of Material Service Safety, University of Science and Technology Beijing, Beijing 100083, China; xiong.haocheng@gmail.com

Abstract

In this study, the feasibility of a novel bottom-up drainage and water pressure reduction system for reducing the secondary lining external water pressure on tunnels has been validated by conducting laboratory evaluations. The tunnels environment including surrounding rock, lining, bottom drainage system and other supplementary components have been simulated to investigate the working pattern and efficiency of this drainage system. The drainage system has been further optimized by analyzing the measured

water pressure and flow rate. Experimental results indicate that the designed draining system is feasible for reducing the secondary lining external water pressure in the bottom of tunnels and the water pressure has been reduced significantly with high efficiency. The capacity of the proposed system to control the rapid water inflow in tunnel construction region can be guaranteed. The factors affecting the performance of the system such as the diameter of the drainage pipe and the inlet water pressure are also discussed in this paper.

1 Introduction

Water penetration and dripping are always critical problems for tunnels in the water-saturated ground. The groundwater in the tunnels are typically treated in two ways: waterproofed or drained (Yoo, 2016). The waterproofed tunnel doesn't allow the groundwater to penetrate the secondary lining as the waterproof boards are set along the circumferential direction to form a complete. This issue very common in urban tunnel constructions due to the low groundwater discharging rate. A drained tunnel usually allows groundwater into the tunnel, which is finally discharged along with the various measures in such tunnel. Usually, the waterproof and drainage system of a drained tunnel consists of initial support, secondary lining, waterproof boards, blind tubes, and central drainage ditches. Existing waterproof and drainage system for tunnels is mainly designed to deal with the groundwater pressure applied on the upper structure of the tunnel (Yuan et al., 2000; Shin et al., 2009). The water pressure applied is supposed to be bearded by the tunnel invert. Unfortunately, it's been proved that the current design is not able to solve the problems due to the potential damages on the ballast bed, including uplift, mud pumping, cracking and so on (Butscher et al., 2017). Among the four causes (Gamisch et al., 2005) of these damages, the groundwater plays a much more important role than the other factors, such as construction defection, long-term train vibration load, and poor surrounding rock.

Many researchers have investigated how to control the external water pressure on the tunnel lining. Arjnoi et al. (2009) conducted theoretical analysis and numerical

simulation to study the effect of drainage conditions on pore water pressure distributions and lining stresses in a drained tunnel with two different boundary conditions. Wang et al. (2008) presented a theoretical model to predict the distribution of water pressure on tunnel lining by laboratory test and field evaluation. Fang et al. (2016) developed an apparatus to apply the appropriate external water pressure by evacuating the inner space of the tunnel and applying external air pressure to the liner to act as the water pressure. Stripple et al. (2016) presented a new design of drainage system for rock tunnels. Yee et al. (2015) and Yee (2015) analyzed the influence between magnetic fields and calcium carbonate deposition through laboratory tests and field evaluations to prevent clogging. Besides, wave vibrations (Xin et al., 2018), Quantum Stick (Jung et al., 2013) and geosynthetic (Jang et al., 2015), etc. were also investigated. Choi et al. (2015) proposed an optimal lightweight-foamed mortar mix suitable for composite lining method to facilitate tunnel drainage. The lightweight-foamed mortar replaces the traditional initial support, and the drainage system works more efficiently due to its porous structure. The current studies mainly focus on the porewater pressure distributions on the whole tunnel lining or the water pressure that applies to the upper structure of the tunnel. There is still much research needs on the solution of the problems occurred on tunnel invert caused by high water pressure.

To prevent the damage of the tunnel invert caused by water pressure, Li et al. (2018) developed a novel bottom-to-up drainage and water pressure reduction system (Fig. 1) to reduce the water pressure that applies on the secondary lining. Such system includes

a transverse catchment system, a longitudinal water conducting system, and a bottom-to-up water drainage system. Series of numerical analyses has been conducted to evaluate its drainage performance. Better waterproof and drainage function can be achieved on the entire tunnel by combining the new and existing technologies.

This paper presents an experiment-based study on the bottom-to-up drainage and water pressure reduction system. The performance of the proposed system will be validated by experiments. The drainage efficiency of different types of drainage pipe and the influence to seepage field caused by the pipe diameter will also be analyzed. The overall idea of this article is shown in flowchart 2.

2 Experimental setup

The equipment setup is shown in Fig. 3 including the structure of tunnel invert, the bottom-to-up drainage, water pressure reduction system and surrounding rock with groundwater, which simulates the structure part highlighted in Fig. 1. According to functions of the components, they can be divided into two systems: water supply system and drainage system. (Water tank(I), Water pump(II), Intake pipe(III), Return pipe(IV), Return valve(V), Inlet valve(VI), Pressure valve(VII), Buffer box(VIII), Inlet holes(IX), Gravel filling(X), Precast concrete board(XI), Convex hull drainboard(XII), Cast-in-place concrete filling(XIII), Half-round tube(XIV), Waterproof board(XV), Gravel filling Ⅱ (XVI), Cover plate(XVII), One-way valve(XVIII), Oblique drainage pipe(XIX), Erect drainage pipe(XX), Studdle(XXI), Ball valve(XXII).)

2.1 Water supply system

The water supply system (Fig.4) consists of 6 parts, providing power to make water flow and receiving water from the drainage system. Water tank(I) is a steel cylinder, which is 1.2m high with an inner diameter of 0.6m and a 2mm-thick wall. The Water pump(II) is the main power supply of the experiment to make water flow, which is 1.1m-long with a flow of 3 m^3/h. Intake pipe(III) connects the water supply system and the simulating drainage system. There are two tees in the intake pipe(III), the first tee divides the flow path into two: one connects inlet valve(VI) to make water flow into the simulating drainage system, the other connects return valve(V) and return pipe(IV) to make water flow back into water tank(I); the second tee divides the other flow path into two to connect testing chamber as there are two intakes on both sides of the testing chamber.

The following two flow paths were designed in this experiment:

1. Path 1 is 1-water tank →2-water pump →3-intake pipe →the first tee →5-return valve →4-return pipe →1-water tank;
2. Path 2 is 1-water tank →2-water pump →3-intake pipe →the first tee →the second tee →6-inlet valve →the simulating drainage system →1-water tank. The volume of water flowing into the testing chamber can be controlled by regulating 5-return valve and 6-inlet valve, the water pressure in the testing chamber can also be controlled if superadding regulating 22-ball valve.

2.2 Drainage system

The drainage system makes up the testing chamber and the components in it. The

113 testing chamber is a cuboid steel box with a size of 3m×1m×0.65m (length × width ×
114 height), which is used to simulate the tunnel invert structure and groundwater shows in
115 Fig.5. There is a buffer box(VIII) in each side of the testing chamber, and the size of
116 the buffer box(VIII) is 0.2m×1m×0.65m (length × width × height). The surplus space
117 of the testing chamber is the main container of simulating tunnel invert. The size of the
118 testing chamber is 2.6m×1m×0.65m (length × width × height). There is a pressure
119 gauge(VII-a) connected to the top of each buffer box(VIII). The Cover plate(XVII) is
120 installed on the top of the testing chamber by screws. The Cover plate(XVII) is
121 manufactured with two parts to reduce the weight for easy transport. On each plate,
122 there is a hole corresponding to the erect drainage pipe and oblique drainage pipe.
123 The components in the testing chamber are shown in Fig.6. From bottom to top,
124 there are gravel filling(X), precast concrete board(XI), convex hull drainboard(XII),
125 cast-in-place concrete filling(XIII), half-round tube(XIV), waterproof board(XV) and
126 gravel filling Ⅱ(XVI), corresponding to the simulation of surrounding rock, initial
127 support, convex hull drainboard, secondary lining, half-round tube and waterproof
128 board on the edge in the bottom-to-up drainage and water pressure reduction system
129 respectively. The permeability of initial support is relatively high in the tunnel because
130 it is usually fabricated by shotcrete. It is very difficult to reproduce the shotcrete support
131 in the laboratory with the same permeability performance. Therefore a gap about 3cm
132 wide is put between two 11-precast concrete boards for water flowing through to reach
133 a permeability similar to the real condition. Gravel filling Ⅱ(XVI) is used to fill the

space between the cast-in-place concrete filling(XIII) and cover plate(XVII) and transfers force if necessary.

There are two types of bottom-to-up drainage pipes: oblique drainage pipe(XIX) and erect drainage pipe(XX). The performance of the drainage pipe can be analyzed through the data of water discharge and water pressure reduction, which helps to improve the design of bottom-to-up drainage and water pressure reduction system in tunnels.

The diameter of the half-round tube(XIV) is 200mm, and that of oblique drainage pipe(XIX) and erect drainage pipe(XX) is 100mm. There are convex parts on both sides of convex hull drainboards(XII). When convex hull drainboard（XII） is set on precast concrete boards(XI), there are plenty of flowing paths under the convex hull drainboard, and the depression area will be filled by cast-in-place concrete to meet the force-bearing demand. The half-round tube is connected to drainage pipes with a tee and waterproof glue. The edges of the waterproof board, half-round tube, and testing chamber will be connected to each other by waterproof glue. The whole structure of the waterproof board, half-round tube, and drainage pipe are shown in

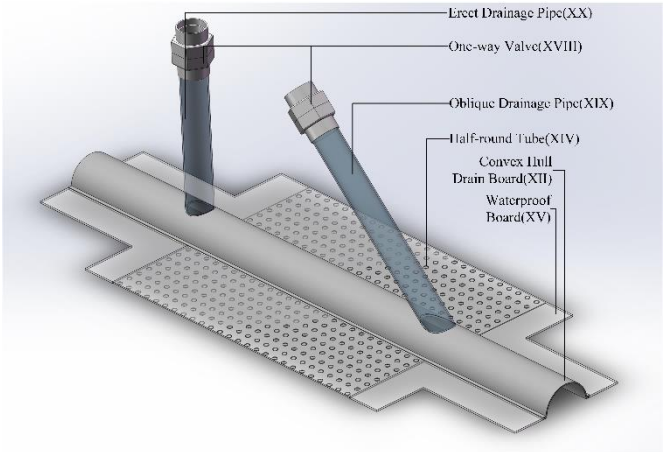

Fig. 7.

3 Monitoring and data acquisition system

In this experiment, the pore water pressure and flow charge of drainage pipes are investigated.

3.1 Pore water pressure monitoring

There are two types of pore pressure sensors: HC-25 micropore pressure sensor (0.2% in precision) and HCYB-25 micropore pressure sensor (0.5% in precision). HCSC-16 data acquisition equipment and YBY-2001 strain acquisition instrument were used for data acquisition. There are 3 tiers of pore pressure sensors installed at different heights (see Fig.). The Bottom Tier Sensors is placed in the gravel filling(X) to monitor the pore pressure representing surrounding rock. The Medium Tier Sensors is placed between precast concrete boards(XI) and waterproof board to monitor the pore pressure that representing simulating secondary lining. The Top Tier Sensors is placed in each drainage pipe which is 15cm higher than the medium tier. The horizontal arrangement of each tier of pore pressure sensors is shown in Fig. . No.1~No.9 sensors are HCYB-25 micro pore pressure sensors, and No.10~No.22 sensors are HC-25 micro pore pressure sensors.

3.2 Water discharge monitoring

Water discharge monitoring system consists of a water container, an electronic scale, and a stopwatch. The weight of the water container was measured before the experiment. When adding water into the container, the corresponding elapsed time was

also monitored. The water discharge of each drainage pipe was obtained by calculating the mass of the water in the container and the elapsed time. For better accuracy, 3 was used as an average value of water discharge in each experimental condition.

4 Experimental programme

4.1 The process of installation of experimental equipment

The process of installing the bottom-to-up drainage and water pressure reduction system for tunnels include filling gravel material, arranging and setting pore pressure sensors, installing drainage pipes, pouring concrete for simulating tunnel invert secondary lining, installation of inlet/outlet pipes and valves, testing of data acquisition equipment and so on. The detailed process is as follows:

(1) Transporting and fix the testing chamber and water tank etc. in the prepared testing field;

(2) Laying some non-woven fabric to cover the inlet holes to prevent any gravel getting into the buffer box;

(3) Filling gravel in the bottom of testing chamber with a thickness of 18cm, tamping to dense the gravel;

(4) Placing the Bottom Tier Sensors according to the prepared arrangement;

(5) Placing two precast concrete boards into the testing chamber and reserve a 3cm gap between them, seal the edge of the boards with waterproof glue;

(6) Placing the Medium Tier Sensors and gather all the wires of the sensors with a tarp;

(7) Installing half-round tube, convex hull drainboard, waterproof board and so on, connect and seal with waterproof glue;

(8) Installing the erect drainage pipe and oblique drainage pipe, set the Top Tier Sensors;

(9) Pouring self-compacting concrete with a thickness of 40cm, tamping gently and complete maintenance;

(10) Filling the upper gravel with a thickness of 10cm and tamping;

(11) Installing the cover plate and connecting it to the testing chamber with screws;

(12) Installing one-way valve, ball valves and other pipes;

(13) Installing intake pipe, valves, water pump and so on, connect the water supply system and the testing chamber;

(14) Installing the pressure gauges on both sides of the testing chamber, connecting sensors and the data acquisition equipment, debugging facilities, and prepare to carry out the experiment.

Fig. shows the entire experimental system.

4.2 Simulations

The following experiments will be discussed in this section.

(1) Steady seepage test

The distribution of water pressure in steady seepage will be analyzed in this study. When performing the experiment, all intake pipes and 4-return pipe will be opened except the drainage pipes, which are controlled by the ball valves(XXII). It includes

three conditions:

Only the ball valve of erect drainage pipe is opened, and the draining is conducted using erect drainage pipe (called “DEDP” for short);

Only the ball valve of oblique drainage pipe is opened, and the draining is conducted using oblique drainage pipe (called “DODP” for short);

Both ball valves are opened, and the draining is conducted using drainage pipes (called “DBDP” for short).

(2) Influence of the drainage pipes diameter on the effect of water pressure reduction

The effect of the water pressure reduction system will be evaluated, and the influence of the diameter of the drainage pipe will also be investigated. Due to the limitation of the laboratory instrumentation, the drainage pipe was not able to be replaced directly to complete the experiment of the diameter of the drainage pipe. Different opening angles of the ball valve(XXII) result in different drainage discharge of the drainage pipe, which is similar to draining with different diameters of drainage pipes. In the experiment, return valve(V) was opened, and the inlet valve(VI) and the ball valve(XXII) was closed. The water pump(II) and the inlet calve(VI) opened gradually to increase the water pressure of the pressure gauge(VII) until 20kPa. The ball valve(XXII) of erect drainage pipe was then opened to about 30°, and the water pressure was measured during the process of the water pressure reduction. This process was repeated, and the water pressure was recorded with ball valve(XXII) of erect

drainage pipe opened to 15° and 10°, and ball valve(XXII) of oblique drainage pipe opened to 30°, 15°, and 10°.

It is found that the inner diameter of the drainage pipe is 10cm when the ball valve(XXII) is opened to about 30°, 15°, and 10°. The equivalent diameters of the drainage pipe are 47mm, 27mm, and 18mm, respectively.

(3) Influence of inlet water pressure on the seepage field

In this section, the water pressure and water discharge will be discussed. The cross-section area of the two types of drainage pipe is as identical as possible to make the inlet water pressure the only variable. In the experiment, the return valve(V) was opened first, then the inlet valve(VI) was closed, and the ball valves(XXII) was then opened to about 10°. The water pump(II) was then started, and the inlet valve(VI) was opened gradually to make the water pressure to reach 5kPa, 10kPa, 15kPa, and 20kPa, which is monitored by pressure gauge(VII). Then the pore water pressure and water discharge of each pressure is obtained.

5 Results and analysis

5.1 Water pressure distribution of steady seepage

In Fig. (a) and Fig. (b), the water discharge of the erect drainage pipe approximately equals to that of the oblique drainage pipe. The exact water discharge values measured from an erect drainage pipe and oblique drainage pipe are 1384.64g/s and 1248.97g/s respectively. The water discharge of erect drainage pipe is slightly greater than that of the oblique pipe. Fig. (c) shows the water discharge of both drainage

pipes during draining. The measured water discharges of erect and oblique drainage pipe are 695.82g/s and 387.24g/s respectively. It is found that, under the same test condition of intake water pressure and opening angles of ball valves, the drainage efficiency of the erect drainage pipe is better than the oblique pipe. It may be due to the difference of the drainage paths since the drainage path of the erect drainage pipe is much shorter than the oblique drainage pipe.

The water pressure values measured by each tier of sensors are shown in **Error! Reference source not found.**, 2, and 3. Comparing to the value monitored by each sensor under different test conditions, the water pressure of most DEDP is less than that of DODP. It means that the water pressure reduction effect of the erect drainage pipe is greater than the oblique drainage pipe, which agrees well with the result proved by water discharge analysis. The water pressure values of most DODP are less than that of the DEDP since the active drainage area of DODP is larger than that of DEDP or DODP. It shows that in a certain range, multiple drain outlets are more conducive to reduce water pressure than a single drain outlet. It indicates that the distance between the two drain outlets needs rational design.

From each tier of sensors, the water pressure measured has a similar trend. It indicates that the water pressure is well distributed and changed synchronously, which proves that the bottom-to-up drainage and water pressure reduction system is effective to reduce water pressure at the bottom of the tunnel. Since the average values of water pressure under each test condition are different, the standard deviation is unable to

validate the data. Therefore, the coefficient of variation ("CV," the ratio of the standard deviation to average value) is chosen to validate the collected data. Only the CV values of the Bottom Tier Sensors in each test condition are more than 10%, which means that the water pressure at the bottom of the testing chamber flutters obviously. The maximum CV value of the Medium and Top tier is 6.10%, which means that the water pressure values in the position of each tier are almost not fluctuant, proving the good distribution of water pressure in another way. The reasons of such fluctuation can be concluded as: 1) The water flow paths are disordered and the flow rate is not as uniform as the bottom tier of pore pressure sensors placed in gravel filling, in which there are plenty disordered interspace; 2) The data measured by the bottom and the top tier of sensors have much better accuracy than the bottom tier.

Under the same condition, the average pore pressure measured from the bottom tier sensors is the highest. The one from the medium tier is lower than the bottom tier, and the one from the top tier is the lowest. The difference of the data measured by the bottom tier and the medium tier, the medium tier, and the top tier is 0.961kPa, 0.896kPa, respectively. The difference is almost the same as the hydrostatic pressure of the sensors in the different height of, which indirectly proves the correctness of these water pressure data.

5.2 Influence of the diameter of the drainage pipe

The water pressure of the secondary lining of the tunnel is primarily affected by

298 the water pressure reduction system. The water pressure measured by No.10~No.22
299 pore pressure sensors is more accurate than No.1~No.9. Therefore, the water pressure
300 data measured by No.10~No.22 sensors will be mainly discussed in this part. The
301 measured water pressure is shown in Table 4. Due to the error of the data acquisition
302 system, the water pressure measured by the 7-pressure gauge varies slightly around
303 20kPa, which should maintain stable at 20kPa accurately without system error.

304 Table 4 shows that when the equivalent diameters are 47mm, 27mm, and 27mm,
305 the water pressure decrease for about 60%, 45%, and 30%, respectively, which indicates
306 that the water pressure decreases with the increase of the equivalent diameter of
307 drainage pipe. This result proves that if the drainage capacity of the drainage and water
308 pressure reduction system is enough for a tunnel, the water pressure on the secondary
309 lining will not increase too much, which agrees with the conclusion of Li (2018). If the
310 drainage capacity of the drainage pipe for a tunnel is not enough for the water inflow
311 of the construction region, the effect of the bottom-to-up drainage and water pressure
312 reduction system will decrease, and it may even result in the damage of the tunnel due
313 to the additional drainage measures in the bottom of the tunnel.

314 The reduction of water pressure due to the influence of drainage pipe diameter is
315 shown in Fig.. When 22-ball valve is opened to about 45° (the equivalent diameter is
316 63mm), the water flow is in a critical state between whole pipe flow and partly-filled
317 pipe-flow, which indicates that the water pressure state approaches to that of opening
318 ball valve about 90°. So the water pressure data of fully opened ball valve will be

319 regarded as that of 45°. And the angle of 0° means the ball valves fully closed, i.e.,
320 water pressure will not decrease.

321 In Fig., with the increase of the equivalent diameter of the drainage pipe, the water
322 pressure reduction ratio gradually increases and tends to be stabilized. For the case that
323 the initial pressure about 20kPa, the water pressure reduction ratio is approximately
324 60%. If the equivalent diameter is larger than 63mm, the whole pipe flow in each pipe
325 will switch to partly-filled pipe-flow. It indicates the water pressure will not decrease
326 any more even if increasing the diameter of the drainage pipe if the initial pressure is
327 20kPa. Therefore, the effect of reducing water pressure on tunnel secondary lining will
328 be better with the increase of drainage pipe diameter as long as it is whole pipe flow.
329 For a certain tunnel region, the whole pipe flow will become partly-filled pipe-flow
330 when the diameter of drainage pipe increases to a certain extent, which means the effect
331 of pressure reduction will not get better any longer. Therefore, for a safe tunnel structure,
332 in the design of the bottom drainage system for the tunnel, the drainage pipe should be
333 large enough for the water inflow of the tunnel construction region.

334 The data of Table 4 and Fig. shows that both the erect and oblique drainage pipe
335 has good performance in water pressure reduction. However, under the same test
336 condition, the water pressure reduction ratio of the erect drainage pipe is more than the
337 oblique drainage pipe for about 4%. It indicates that the drainage effect of erect drainage
338 pipe is better than the oblique drainage pipe to some extent.

339 The data of No.15 pore pressure sensor monitoring water pressure decreasing

process is shown in Fig.. The water pressure decreasing process of both erect and oblique drainage pipe is great, which lasting about 2~3s, when the equivalent diameters are 47mm and 27mm. The water pressure of the pipe with an equivalent diameter of 18mm decreases very slowly, after about 50s the water pressure still shows some trend to decrease. This experimental phenomenon indicates that a large enough cross-section area of the drainage pipe contributes to a more rapid water pressure reduction process, which is helpful to deal with the sudden increase of water pressure like a sudden rainfall. Contrarily, if the diameter of the drainage pipe is too small, the water pressure decreases rapidly at first and then very slow, which leads to a long drainage process with little effect. Thus, it is critical to have a large enough drainage pipe to satisfy the requirement of the tunnel structure. It is not necessary to use a partly-filled pipe-flow while a whole pipe flow can reduce water pressure on the secondary lining of a tunnel efficiently. The changing curve of water pressure with a time of 27mm-equivalent-diameter erect drainage pipe and 27mm-equivalent-diameter oblique drainage pipe is shown in Fig.. With a comprehensive consideration of security, cost-effectiveness, etc., it is recommended that the drainage capacity should be designed for a partly-filled pipe-flow for the dry season and a whole pipe flow for the rainy season.

5.3 Influence of inlet water pressure

The relationship between water pressure and intake water pressure is shown in Fig.. The water pressure increases linearly with the increase of intake pressure, which

361 is similar to the results of the study by Li et al. (2018). It shows that the secondary lining
362 external water pressure increase approximately identically as the increase of water head
363 height of the vault. Since the pore pressure sensors and the pressure gauges are placed
364 at different locations in this study, the data measured from them be used to validate each
365 other. All the water pressure values are shown in Fig. have a similar trend which
366 indicates that there is no sudden change of pressure observed in the experiment. It
367 demonstrates that the simulation of the steady seepage and monitoring methods of water
368 pressure change in this study is feasible, and the water pressure is well distributed with
369 no serious fluctuation.

370 The influence of intake pressure on the flow rate is shown in Fig.. The flow rate is
371 measured in the steady flow, and the cross-section area of both types of drainage pipes
372 are the same, meaning the difference of flow rate should only be caused by the drainage
373 pipe types. Fig. shows a linear relation of the flow rate and the inlet water pressure. The
374 flow rate increases with the increase in intake pressure. The flow rate of the erect
375 drainage pipe is two times higher than the oblique drainage pipe with the same intake
376 pressure. Therefore, it can be concluded that with the same cross-section area and whole
377 pipe flow, the flow rate of the erect drainage pipe is about two times greater than the
378 oblique drainage pipe. Furthermore, the slope of the flow rate curve of the erect
379 drainage pipe is much larger than the oblique drainage pipe. It indicates that the water
380 discharge of the erect drainage pipe would increase rapidly with the increase of the
381 intake pressure. In other words, the erect drainage pipe can manage the sudden change

382 of the water inflow more efficiently. Therefore, the erect type of drainage pipe is more
383 effective than the oblique type in the water flow rate analysis.
384
385 **6 Summary and Conclusion**
386 This paper presents a study on assessing the feasibility of bottom-up drainage and
387 water pressure reduction system for railway tunnels by simulation and analyzing the
388 pressure reduction effect. The experiment equipment consists of two main parts: the
389 water supply system and the drainage system. The experiment was set up imitating the
390 bottom structure of the tunnel with the bottom drainage system under three test
391 conditions: water pressure distribution of steady seepage in a regular working state; the
392 influence of the change of the drainage pipes diameter on the effect of water pressure
393 reduction; and inlet water pressure on the seepage field. The results of the experiment
394 can be summarized as follows:
395 (1) The bottom-up drainage system can effectively drain the water in the bottom
396 of the tunnel by the difference of natural hydraulic pressure.
397 (2) It is discovered that the erect drainage pipe is better than the oblique one in the
398 drainage efficiency, flow rate, and percentage reduction of water pressure.
399 (3) The bottom-up drainage and water pressure reduction system can effectively
400 reduce the secondary lining external water pressure, and there will be a well water
401 pressure distribution at the bottom of the tunnel.
402 (4) If the water inflow is stable with whole pipe drainage, the reduction effect of

403 water pressure is remarkable by increasing the diameter of the drainage pipe. In
404 other words, if the drainage pipes are incapable of draining the water at the bottom
405 of tunnels, the reduction effect of water pressure on the secondary lining is
406 unremarkable, and the reduction process is very long.
407 (5) In the design of drainage pipes, the safety of the tunnel lining structure needs
408 to be taken into consideration and guarantee as well as the water inflow difference
409 of rainy season and dry season. Therefore, the design of partly-pipe flow in the dry
410 season and whole pipe flow in the rainy season is recommended.
411 This study proved the bottom-to-up drainage and water pressure system is feasible
412 for use on tunnels. Due to the difference between the construction site and laboratory
413 test, more field test data is necessary to validate and optimize the performance of the
414 proposed drainage system.
415

416 **Acknowledgments**

417 The support of project of research and development of science and technology
418 from CHINA RAILWAY (CR) with Grant No. 2016G002-O and Grant No. 2014G004-
419 C is highly appreciated.
420

421 **Reference**

422 Arjnoi, P., Jeong, J., Kim, C., Park, K., 2009. Effect of drainage conditions on porewater pressure
423 distributions and lining stresses in drained tunnels. Tunn. Undergr. Sp. Technol. 24, 376–

389. https://doi.org/10.1016/j.tust.2008.10.006

Butscher, C., Scheidler, S., Farhadian, H., Dresmann, H., Huggenberger, P., 2017. Swelling potential of clay-sulfate rocks in tunneling in complex geological settings and impact of hydraulic measures assessed by 3D groundwater modeling. Eng. Geol. 221, 143–153. https://doi.org/10.1016/j.enggeo.2017.03.010

Choi, H., Ma, S., 2015. An optimal lightweight foamed mortar mix suitable for tunnel drainage carried out using the composite lining method. Tunn. Undergr. Sp. Technol. 47, 93–105. https://doi.org/10.1016/j.tust.2014.12.002

Fang, Y., Guo, J., Grasmick, J., Mooney, M., 2016. The effect of external water pressure on the liner behavior of large cross-section tunnels. Tunn. Undergr. Sp. Technol. 60, 80–95. https://doi.org/10.1016/j.tust.2016.07.009

Gamisch, T., Girmscheid, G., 2005. Future trends in construction and maintenance management of drainage systems in traffic tunnels. In: 12th Australian Tunnelling Conference, Brisbane, Australia.

Jang, Y.-S., Kim, B., Lee, J.-W., 2015. Evaluation of discharge capacity of geosynthetic drains for potential use in tunnels. Geotext. Geomembranes 43, 228–239. https://doi.org/10.1016/j.geotexmem.2015.03.001

Jung, H., Han, Y., Chung, S., Chun, B., Lee, Y., 2013. Evaluation of advanced drainage treatment for old tunnel drainage system in Korea. Tunn. Undergr. Sp. Technol. 38, 476–486. https://doi.org/10.1016/j.tust.2013.08.004

Li, P., Liu, H., Zhao, Y., Li, Z., 2018. A bottom-to-up drainage and water pressure reduction

445 system for railway tunnels. Tunn. Undergr. Sp. Technol. 81, 296–305.
446 https://doi.org/10.1016/j.tust.2018.07.027
447 Shin, H.-S., Youn, D., Chae, S., Shin, J., 2009. Effective control of pore water pressures on tunnel
448 linings using pin-hole drain method. Tunn. Undergr. Sp. Technol. 24, 555–561.
449 https://doi.org/10.1016/j.tust.2009.02.006
450 Stripple, H., Boström, L., Ellison, T., Ewertson, C., Lund, P., Melander, R., 2016. Evaluation of
451 two different drainage systems for rock tunnels. Tunn. Undergr. Sp. Technol. 58, 40–48.
452 https://doi.org/10.1016/j.tust.2016.03.015
453 Wang, X., Tan, Z., Wang, M., Zhang, M., Ming, H., 2008. Theoretical and experimental study of
454 external water pressure on tunnel lining in controlled drainage under high water level. Tunn.
455 Undergr. Sp. Technol. 23, 552–560. https://doi.org/10.1016/j.tust.2007.10.004
456 Xin, Z., Moon, J.H., Kim, Y.U., 2018. Reduction of Adherent Forces of Sedimentous
457 Contaminants in Tunnel Drainage using Vibrations from Flexible and Transparent Organic
458 Films. KSCE J. Civ. Eng. 22, 2619–2622. https://doi.org/10.1007/s12205-017-0688-5
459 Yee, E., 2015. Substrate Modification and Magnetic Water Treatment on the Maintenance of
460 Tunnel Drainage Systems. II: Field Tests. J. Perform. Constr. Facil. 29, 04014077.
461 https://doi.org/10.1061/(ASCE)CF.1943-5509.0000575
462 Yee, E., Jang, Y. S., and Chun, B. S. (2014). “Substrate modification and magnetic water treatment
463 on the maintenance of tunnel drainagesystems. Part I: Feasibility tests.” J. Perf. Constr.
464 Facil., 10.1061/(ASCE)CF.1943-5509.0000572, 04014076.
465 Yoo, C., 2016. Hydraulic deterioration of geosynthetic filter drainage system in tunnels – its

impact on structural performance of tunnel linings. Geosynth. Int. 23, 463–480. https://doi.org/10.1680/jgein.16.00010

Yuan, Y., Jiang, X., Lee, C.F., 2000. Tunnel waterproofing practices in China. Tunn. Undergr. Sp. Technol. 15, 227–233. https://doi.org/10.1016/S0886-7798(00)00048-1

Appendix A. Figures

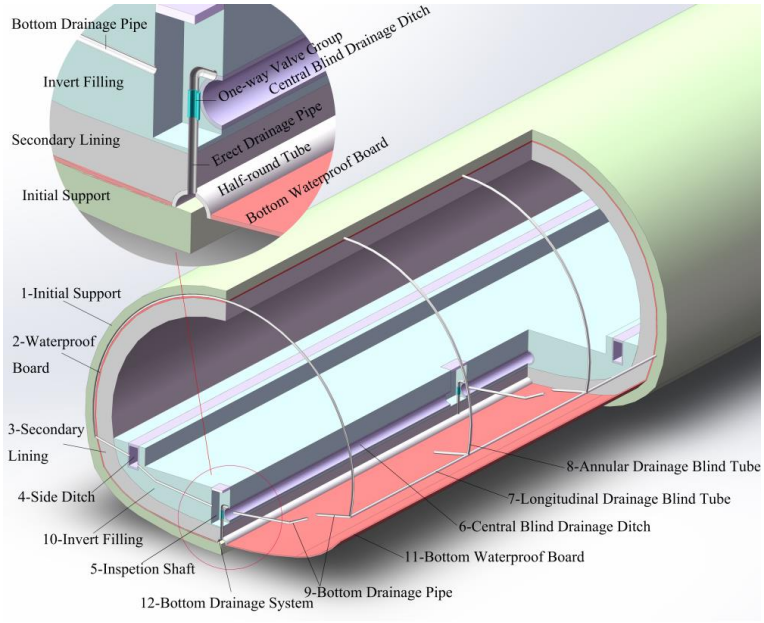

Fig. 1. "bottom-to-up" drainage and pressure reduction system at the bottom of railway tunnels (Li et al., 2018)

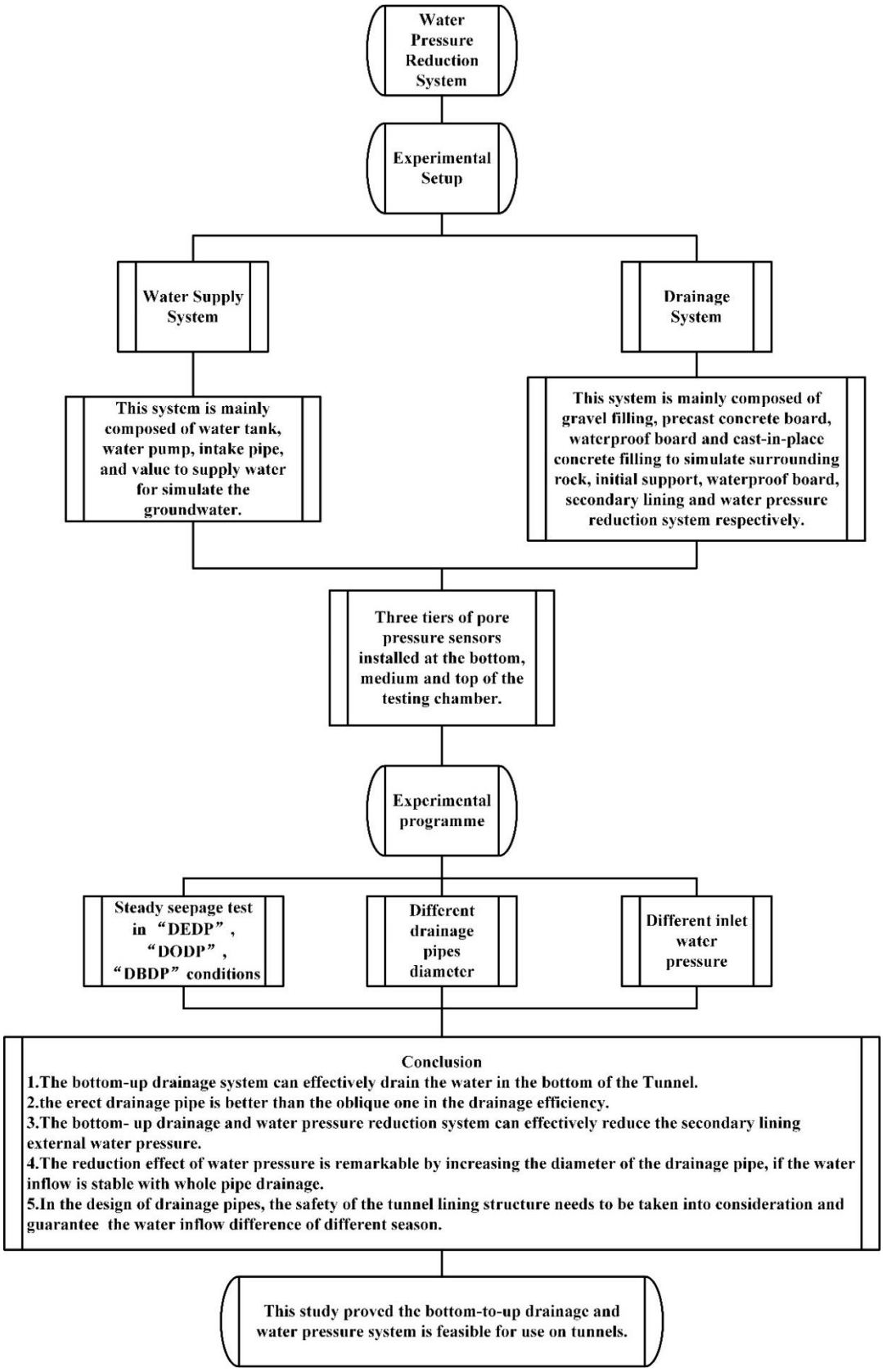

475

476 **Fig. 2. The overall idea flowchart**

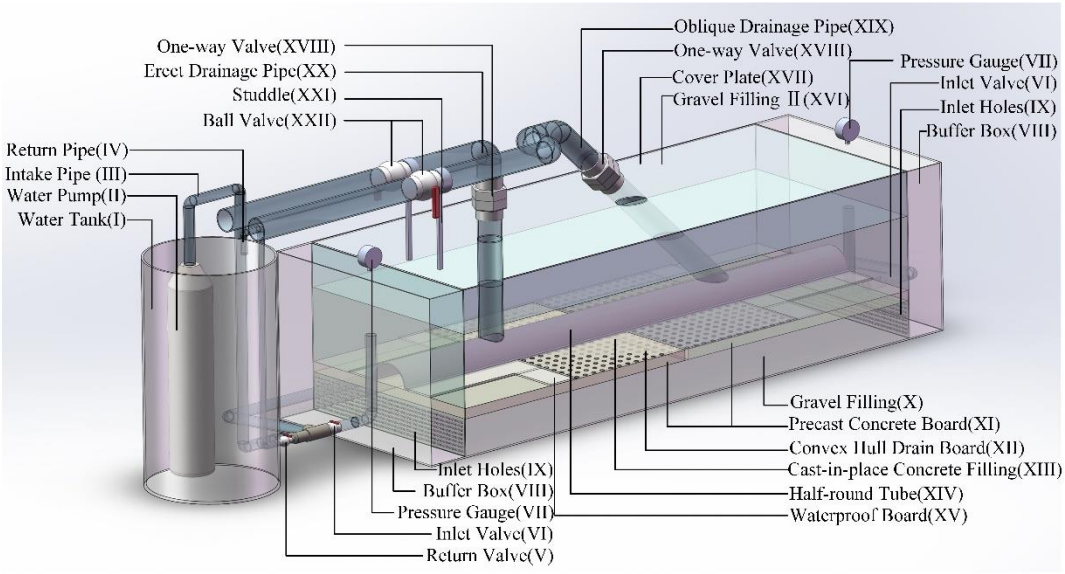

Fig. 3. Sketch of the experimental drainage system

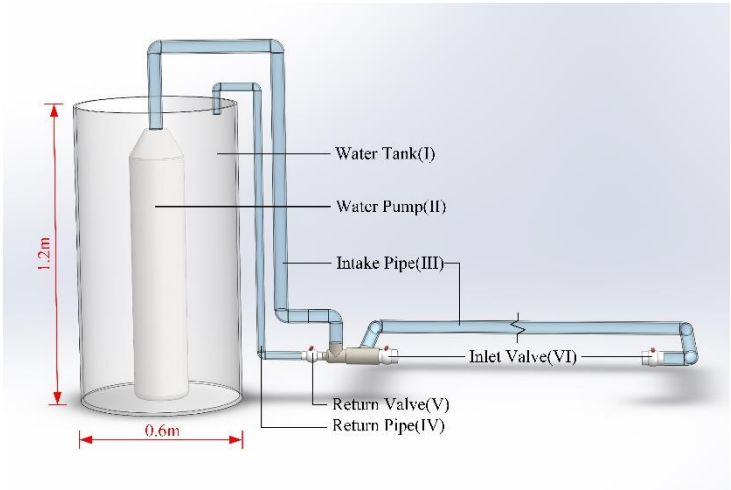

Fig. 4. Sketch of the water supply system

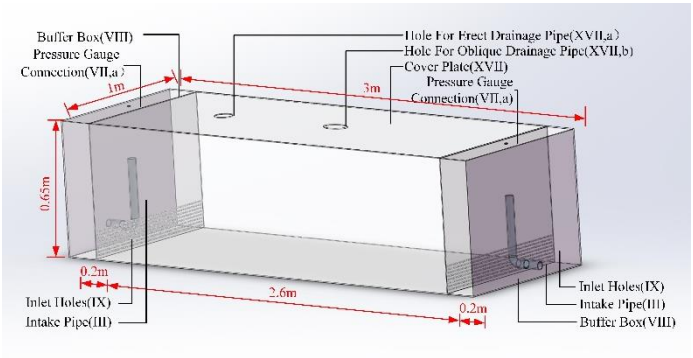

Fig. 5. Sketch of the testing chamber

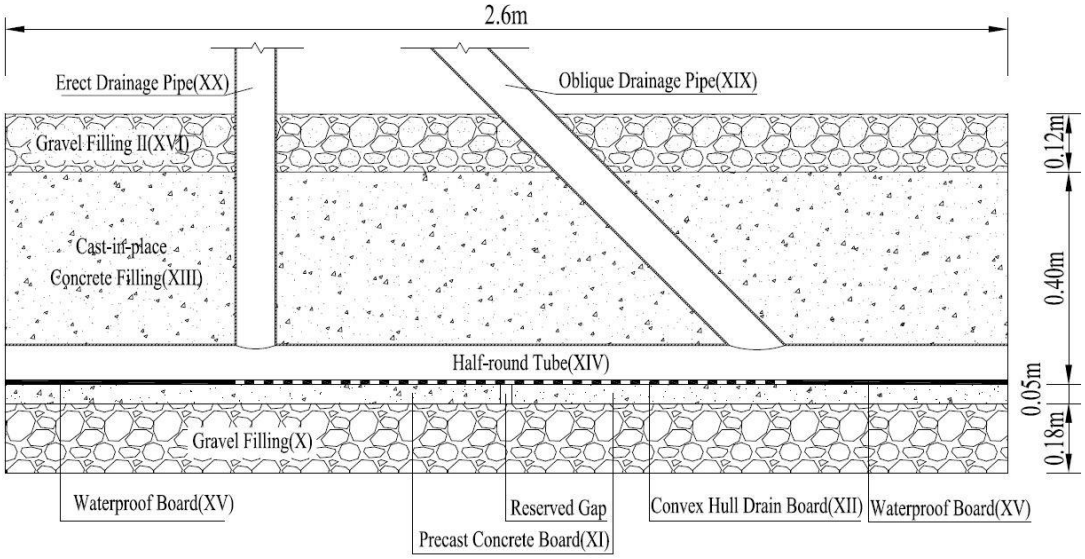

Fig. 6. Sketch of the simulating tunnel invert structure and drainage system in the testing chamber

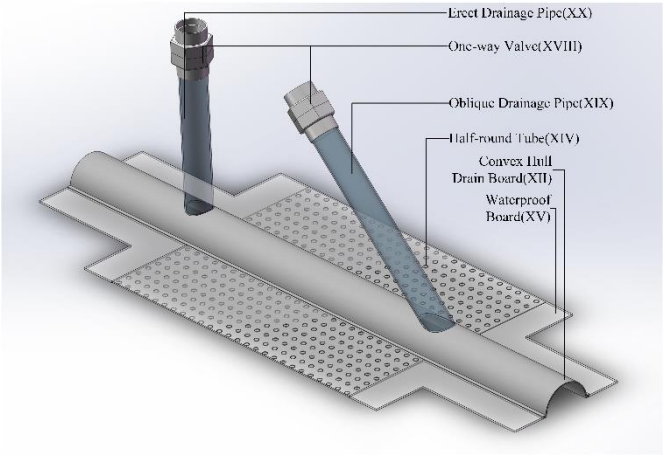

Fig. 7. Sketch of the waterproof and drainage measures

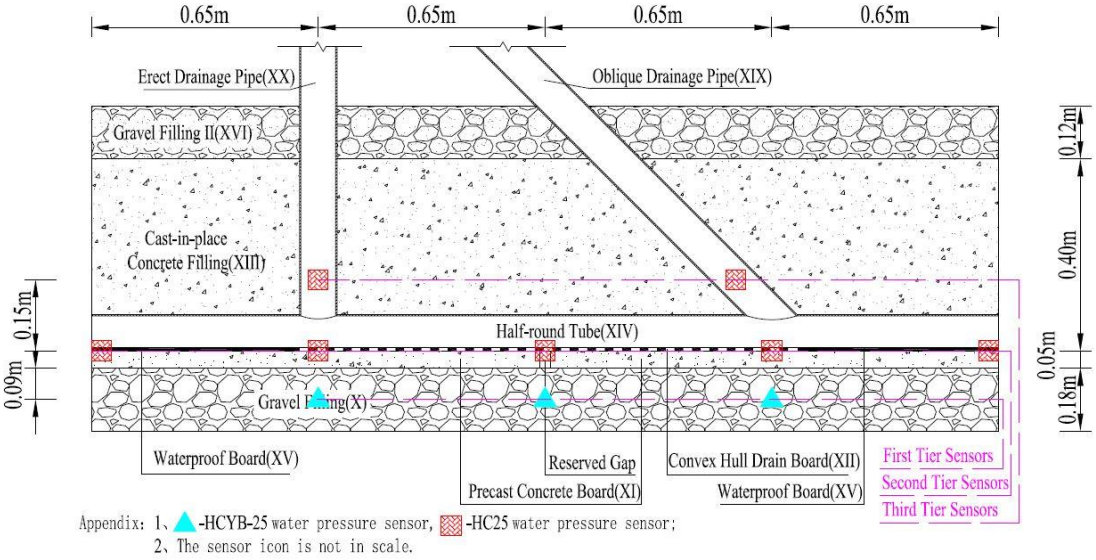

Fig. 8. Vertical sectional profile of the arrange of the pore pressure sensor

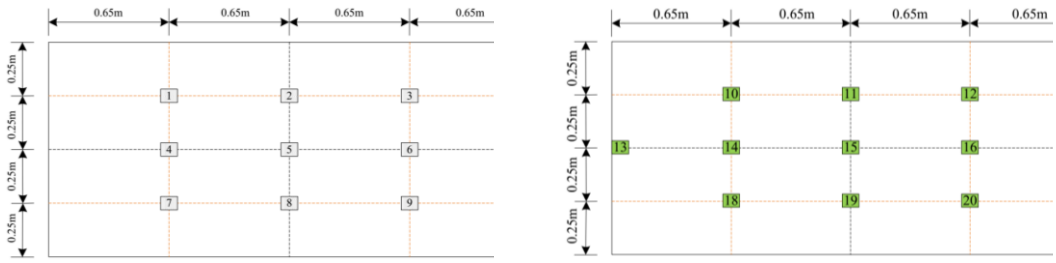

(a) The Bottom Tier Sensors **(b) The Medium Tier Sensors**

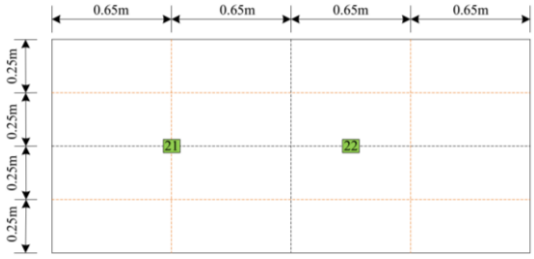

(c) The Top Tier Sensors

Fig. 9. The horizontal arrangement of each tier of the pore pressure sensor

Fig. 10. Photo of the whole prepared experimental equipment

(a) Only drain by erect pipe **(b) Only drain by oblique pipe** **(c) Drain by both pipes**

Fig. 11. Water discharge of the drainage pipe in different test conditions

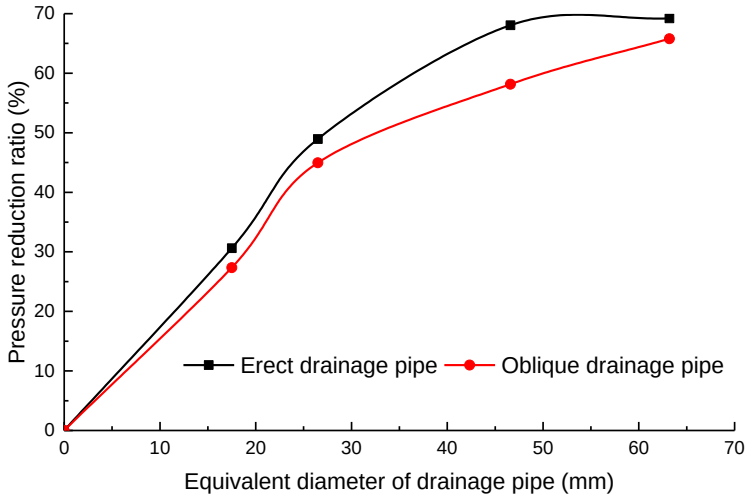

Fig.12. The curve of the water pressure reduction and the equivalent diameter of the drainage pipe

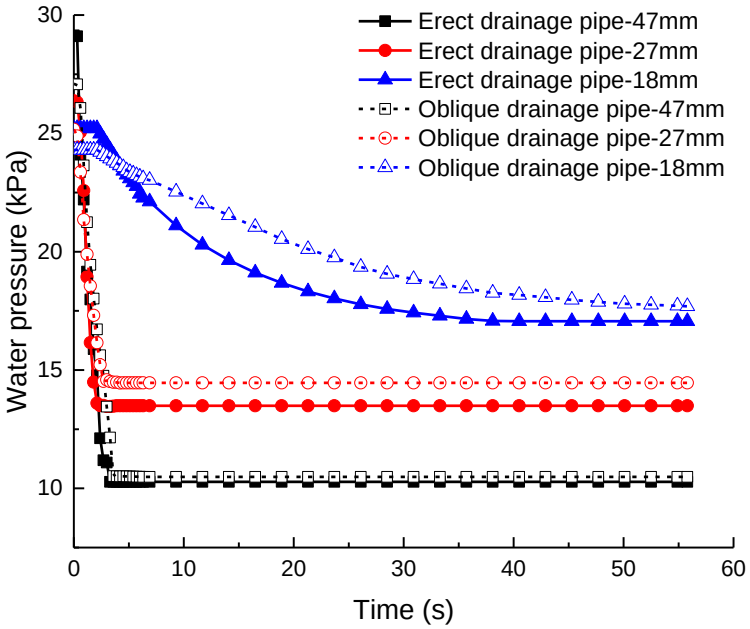

Fig.13. The curve of the water pressure reducing process monitoring by No.15 sensor

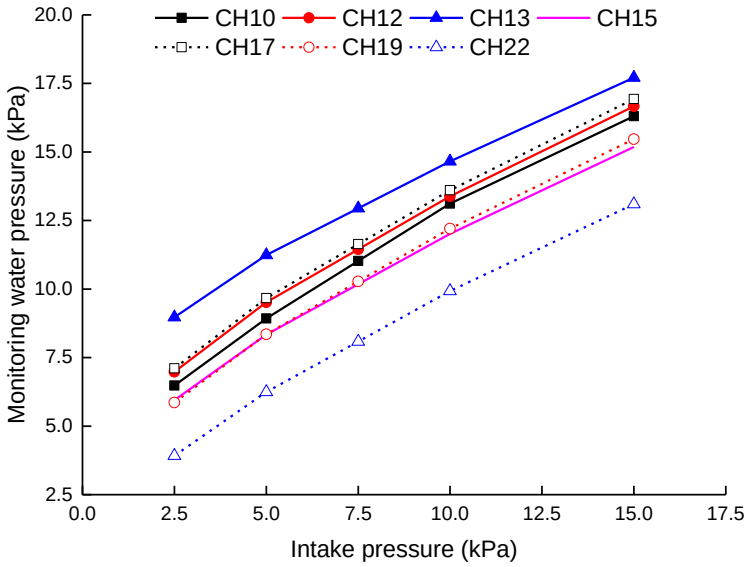

505

506 **Fig.14. Relation curve of monitoring water pressure and inlet water pressure**

507

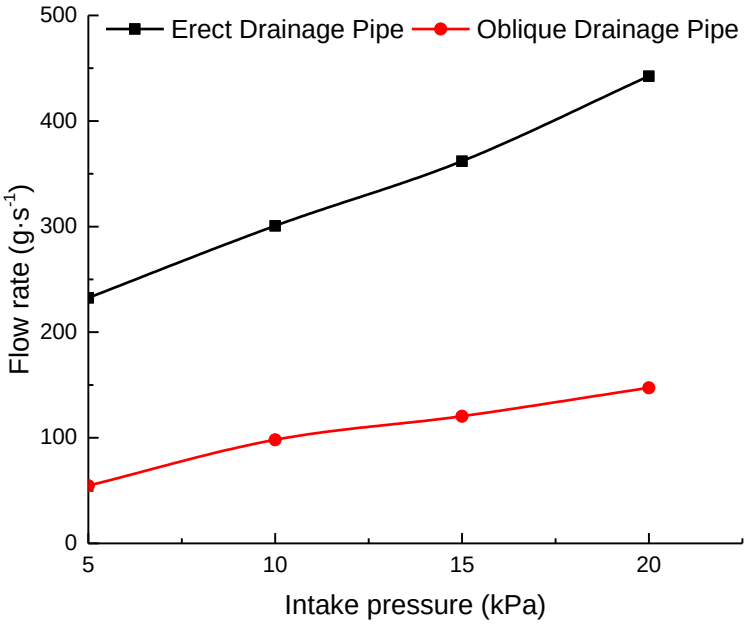

508

509 **Fig.15. Relation curve of flow rate and inlet water pressure**

510

Appendix B.

Table 1 Water pressure measured by the first tier of pore pressure sensors

Item	CH1 /kPa	CH2 /kPa	CH3 /kPa	CH4 /kPa	CH5 /kPa	CH6 /kPa	CH7 /kPa	CH8 /kPa	CH9 /kPa	Average /kPa	Standard deviation /kPa	Coefficient of variation /%
DBDP	10.694	10.161	/*	9.985	11.925	8.490	10.153	10.206	12.044	10.457	1.138	10.88
DEDP	11.450	10.094	/	9.989	10.749	8.204	10.153	10.305	12.047	10.374	1.139	10.98
DODP	13.383	9.835	/	10.212	11.934	9.327	10.389	10.653	10.695	10.804	1.287	11.92

*：“/”means no available data because of sensor damage.

Table 2 Water pressure measured by the second tier of pore pressure sensors

Item	CH10 /kPa	CH11 /kPa	CH12 /kPa	CH13 /kPa	CH14 /kPa	CH15 /kPa	CH16 /kPa	CH17 /kPa	CH18 /kPa	CH19 /kPa	CH20 /kPa	Average /kPa	Standard deviation /kPa	Coefficient of variation /%
DBDP	9.748	9.664	9.653	9.323	9.666	9.361	9.363	9.638	8.575	9.681	/*	9.467	0.351	3.70
DEDP	9.889	9.809	9.798	9.407	9.817	9.588	9.590	9.791	8.197	9.823	/	9.571	0.505	5.28
DODP	10.072	9.987	9.961	9.619	10.000	9.733	9.716	9.962	8.084	10.005	/	9.714	0.592	6.10

*：“/”means no available data because of sensor damage.

Table 3 Water pressure measured by the third tier of pore pressure sensors

Item	CH21 /kPa	CH22 /kPa	Average /kPa	Standard deviation /kPa	Coefficient of variation /%
DBDP	8.629	8.392	8.510	0.167	1.96
DEDP	8.751	8.657	8.704	0.067	0.77
DODP	8.949	8.753	8.851	0.139	1.57

Table 4 Water pressure value and pressure decrease percentage in different diameter of drainage pipe

Equivalent diameter /mm	Drain pipe	Item	CH10	CH11	CH12	CH13	CH14	CH15	CH16	CH17	CH18	CH19	CH20	CH21	CH22	Average
47	Erect drainage pipe	Before	30.766	30.455	30.814	24.736	35.486	29.202	29.083	29.781	28.998	31.228	/*	31.579	27.526	
		After	10.055	9.910	9.901	9.356	10.012	10.276	11.023	10.019	6.776	9.945	/	8.827	8.334	
		Percentage	67.32%	67.46%	67.87%	62.18%	71.79%	64.81%	62.10%	66.36%	76.63%	68.15%	/	72.05%	69.72%	68.04%
	Oblique drainage pipe	Before	28.324	27.997	28.257	23.572	31.171	26.903	26.869	27.641	25.386	28.522	/	28.340	25.036	
		After	10.596	12.050	12.052	11.266	12.169	12.021	12.749	12.137	8.916	12.084	/	10.984	10.046	
		Percentage	62.59%	56.96%	57.35%	52.20%	60.96%	55.32%	52.55%	56.09%	64.88%	57.63%	/	61.24%	59.87%	58.14%
27	Erect	Before	28.564	27.582	27.716	24.605	28.639	26.314	26.560	27.724	/	27.803	/	26.928	24.522	

	drainage	After	14.816	14.253	14.234	13.752	13.851	13.477	13.780	14.552	/	14.216	/	12.941	11.668	
	pipe	Percentage	48.13%	48.33%	48.64%	44.11%	51.63%	48.78%	48.12%	47.51%	/	48.87%	/	51.94%	52.42%	48.95%
	Oblique	Before	26.883	26.190	26.372	22.715	28.192	25.094	25.200	26.114	/	26.558	/	25.945	23.281	
	drainage	After	15.024	14.589	14.603	13.559	14.790	13.852	14.075	14.741	/	14.644	/	13.522	12.049	
	pipe	Percentage	44.11%	44.30%	44.63%	40.31%	47.54%	44.80%	44.15%	43.55%	/	44.86%	/	47.88%	48.24%	44.94%
	Erect	Before	26.739	25.905	26.020	22.996	27.099	24.722	24.935	25.976	/	26.067	/	25.255	22.933	
	drainage	After	18.713	18.091	18.111	16.683	18.329	17.178	17.446	18.290	/	18.079	/	17.004	15.394	
	pipe	Percentage	30.02%	30.16%	30.39%	27.45%	32.36%	30.52%	30.04%	29.59%	/	30.65%	/	32.67%	32.87%	30.61%
18	Oblique	Before	26.356	25.518	25.618	22.742	26.581	24.336	24.568	25.610	/	25.655	/	24.813	22.532	
	drainage	After	19.286	18.636	18.668	17.194	18.885	17.704	17.974	18.847	/	18.634	/	17.569	15.921	
	pipe	Percentage	26.83%	26.97%	27.13%	24.39%	28.95%	27.25%	26.84%	26.41%	/	27.37%	/	29.19%	29.34%	27.33%

523 * : “/” means no available data because of sensor damage.